RSC Advances

ROYAL SOCIETY
OF **CHEMISTRY**

www.rsc.org/advances

Synthesis and characterization of ^{18}F-labeled hydrazinocurcumin derivatives for tumor imaging

Sarah Shin,[ab] Hyun-Jung Koo,[a] Iljung Lee,[a] Yearn Seong Choe,[*ab] Joon Young Choi,[a] Kyung-Han Lee[ab] and Byung-Tae Kim[a]

[†]Department of Nuclear Medicine, Samsung Medical Center, Sungkyunkwan University School of Medicine, 81 Ilwon-ro, Kangnam-ku, Seoul 06351, Korea

[‡]Department of Health Sciences and Technology, SAIHST, Sungkyunkwan University, Seoul 06351, Korea

Submitted to: RSC Advances

*Corresponding author: Tel: +82-2-3410-2623; Fax: +82-2-3410-2667; Email: ysnm.choe@samsung.com

Abstract

Fluorine-substituted hydrazinocurcumin derivative **1** and its dimethyl-substituted form at C2

and C6 positions (**2**) were synthesized and their radiolabeled forms, [^{18}F]**1** and [^{18}F]**2**, were

evaluated for tumor imaging. *In vitro* and *in vivo* metabolism studies showed that the two

radioligands were resistant to reductive metabolism, probably due to the presence of a

pyrazole ring. In the cellular uptake studies, [^{18}F]**1** and [^{18}F]**2** exhibited comparable uptake by

human umbilical vascular endothelial cells and rat C6 glioma cells. Inhibition of radioligand

uptake to a similar extent by HC and curcumin suggests that these radioligands may share the

same binding sites as those for HC and curcumin. Positron emission tomography imaging of

C6 glioma xenografted mice acquired 30 and 60 min after radioligand injection showed that

[^{18}F]**2** had markedly higher tumor uptake than [^{18}F]**1**, which was consistent with

biodistribution data ($3.20 \pm 0.35\%$ ID/g vs. $0.98 \pm 0.31\%$ ID/g, respectively). However, the

two radioligands showed similar levels of tumor-to-background uptake ratios, except for the

significantly higher uptake of [^{18}F]**1** by the small intestines, indicating its more rapid

clearance. The results of this study will guide further structural modifications of these

radioligands to enhance tumor-to-background uptake ratios.

Introduction

It is known that 5-hydroxy-1,7-bis(4-hydroxy-3-methoxyphenyl)-1,4,6-heptatrien-3-one

(curcumin), a major ingredient of the curry spice turmeric, has anticancer, antioxidant, and

antiinflammatory activities.[1,2] Despite its multiple activities, curcumin has poor

bioavailability, which may result from its rapid metabolism in the liver and intestinal walls.[3-5]

We previously synthesized a curcumin derivative substituted with [^{18}F]fluoropropyl group at

one of the 4'-aromatic OH groups for β-amyloid plaque imaging.[6] Despite its suitable

lipophilicity and excellent *in vitro* binding affinity for β-amyloid aggregates,

[^{18}F]fluoropropylcurcumin showed poor penetration through the blood-brain barrier (BBB),

probably due to rapid metabolism of curcumin resulting in formation of its reductive

metabolites, conjugation products, and reductive metabolites with conjugation.

   In addition, curcumin has high reactivity at the central carbon and limited solubility,

therefore, a more stable and hydrophilic derivative, 3,5-bis[*β*-(4-hydroxy-3-methoxyphenyl)-

ethenyl]pyrazole (hydrazinocurcumin; HC) has been synthesized and evaluated for diverse

biological activities. Initial studies of HC demonstrated a more potent inhibitory activity than

curcumin for 5-lipoxygenase (IC$_{50}$ = 1.0 μM vs. 8.0 μM), which converts arachidonic acid to

a host of lipoxygenase products.[7] HC was also shown to have antioxidant, cyclooxygenase

(COX) inhibitory, and antiinflammatory activities, with even higher activity and COX-

2/COX-1 selectivity than curcumin.[8] Its activity has been expanded to the field of neurology; HC showed more potent inhibitory activity than curcumin against calcium/calmodulin-dependent protein kinase II, which is known to be associated with various brain functions including learning and memory,[9] and also exhibited potent activity against multiple targets associated with pathologic biomarkers of Alzheimer's disease.[10] Anticancer activity of HC has been reported, with more potent cytotoxicity (ED_{50} = 1.0 - 3.9 μg/mL) than curcumin against various human cancer cell lines including MCF-7, A549, KB, U87MG, CAKI-1, 1A9, HCT-8, SK-MEl-2, PC-3, HepG2, and LNCaP (clone FGC).[11] Antiangiogenesis activity of HC has also been reported, as shown by its inhibitory activity on endothelial cell proliferation and *in vivo* neovascularization of chorioallantoic membrane.[12] Another study showed that HC was more potent than curcumin in inhibiting signal transducer and activator of transcription 3, which in turn resulted in inhibition of cell proliferation, migration and invasion, and induction of cell apoptosis.[13] A recent study demonstrated that HC was more effective than curcumin for prevention of diethylnitrosamine-induced hepatocarcinogenesis in rats.[14]

Recently, radiolabeled curcumin and HC derivatives were developed for β-amyloid plaque imaging and cancer cellular uptake studies. ^{18}F-labeled HC derivative, 2-[3,5-bis(4-hydroxy-3-methoxystyryl)-1*H*-pyrazol-1-yl]-*N*-{1-[2-(2-(2-[^{18}F]fluoroethoxy)ethoxy)ethyl)-1*H*-1,2,3-triazol-4-yl]methyl}acetamide had low BBB penetration in a WT and transgenic APP23 mice,

even though it labeled β-amyloid plaques of APP23 mouse brain sections using *in vitro* autoradiography.[15] [nat/68]Ga-labeled homodimers of curcumin, diacetylcurcumin, and bis(dehydroxy)curcumin were tested for binding affinity to β-amyloid fibrils and uptake by A549 lung cancer cells.[16]

Unlike curcumin, the *in vivo* effects of HC and its derivatives have not been extensively studied and there are few reports on their metabolism. We recently found that introduction of methyl groups at both C2 and C6 positions of curcumin significantly diminishes reductive metabolism by creating steric hindrance against reductive metabolizing enzymes.[17] In addition, HC as well as curcumin has never been applied to tumor imaging, despite its well-known anticancer activity. In the present study, therefore, we synthesized 4-((*E*)-2-(5-(4-(2-(2-[18F]fluoroethoxy)ethoxy)-3-methoxystyryl)-1*H*-pyrazol-3-yl)vinyl)-2-methoxyphenol ([18F]**1**) and its 2,6-dimethyl derivative ([18F]**2**)*,* elucidate their metabolism, and evaluated them as tumor imaging agents in a C6 glioma xenograft model using micro positron emission tomography (microPET).

Results

Chemistry

We designed and synthesized six fluorine-substituted HC derivatives for development of [18]F-

labeled radioligands for tumor imaging (Fig. 1). HC derivatives (**1-6**) were readily

synthesized by hydrazination of curcumin derivatives (**7-12**) (Scheme 1).[7,12] Curcumin

derivatives (**7-12**) were synthesized using a previously reported method with slight

modifications;[18,19] sequential aldol condensation of 1,3-diketone with one equivalent of

vanillin and then with one equivalent of fluoroalkyl vanillin (**17-19**) was carried out via

coupling of a boron complex of the 1,3-diketone moiety with aldehyde in the presence of

amine, followed by acid treatment of the coupling product. Fluoroalkyl vanillin (**15** and **18-

19**) was synthesized by *O*-alkylation of vanillin using 2-(2-chloroethoxy)ethanol or

fluoroalkyl tosylate in the presence of K_2CO_3 at 100-110 ^{o}C.[20] The hydroxyl group of **15** was

converted into a methanesulfonyl group, which was then reacted with CsF in *t*-BuOH to give

the fluoropegylated vanillin **17**.[21] The *E,E*-configurations of the 2,6-dimethyl groups of **2**

were confirmed by two-dimensional rotating-frame nuclear Overhauser effect spectroscopy

(ROESY) (see 2D ROESY spectra, Supplementary Information).[22-24] These experiments

showed no cross-peaks between methyl protons at C2 and C6 positions (2.30 ppm) and

olefinic protons at C1 and C7 positions (6.98 and 6.99 ppm), indicating that methyl protons

do not exist in close proximity (< 5 Å) in space with both olefinic protons. However, cross-

peaks were observed between methyl protons at C2 and C6 positions and phenyl protons

(6.93, 6.92, and 6.90 ppm) and between the methyl protons and a proton at C4 position (6.58

ppm), indicating that methyl protons at C2 and C6 are on the same side as proton at C4.

Moreover, the intensities of cross-peaks between the methyl protons and aromatic protons

were dependent on the distance between the two protons.[23,25] These data demonstrated that

the dimethyl groups of **2** are in *E,E*-configurations. Based on these results, the 2,6-dimethyl

HC derivatives synthesized in this study (**2**, **4**, and **6**) were assigned to have *E,E*-configurations.

For radiochemical synthesis of [^{18}F]**1** and [^{18}F]**2**, the tosylate precursors **26** and **27** were

synthesized (Scheme 2). Compound **20** was synthesized from **13** and pegylated vanillin **15**; in

this reaction, recrystallization after flash column chromatography was required because

compounds **15** and **20** were not separable on flash column chromatography. Subsequent

hydrazination of the 1,3-diketone moiety of **20** was readily carried out to yield **22**. The bis-

methoxymethyl (MOM) protected precursor, **26** was then used for preparation of [^{18}F]**1**.

Precursor **27** for synthesis of [^{18}F]**2** was prepared as described for synthesis of **26**.

Synthesis of radioligands

[^{18}F]**1** and [^{18}F]**2** were synthesized by reaction of the corresponding precursors (**26** and **27**)

with *n*-Bu$_4$N[^{18}F]F at 110 °C for 10 min followed by removal of the protecting groups in 6 N

HCl at 120 °C for 10 min (Scheme 2). ^{18}F-labeling of the precursors was readily carried out

by protecting the aromatic OH and pyrazole NH groups, unlike the multi-step synthesis of

[^{18}F]fluoropropylcurcumin from 4-(3-[^{18}F]fluoropropoxy)-3-methoxybenzaldehyde and 5-

hydroxy-1-(4-hydroxy-3-methoxyphenyl)-1,4-hexadien-3-one.[6] Subsequent HPLC

purification gave [^{18}F]**1** and [^{18}F]**2** in overall decay-corrected radiochemical yields of 25-35%

and with specific activity of 51.06 GBq/μmol and 44.5 GBq/μmol, respectively.

Measurement of partition coefficient

The partition coefficients of [^{18}F]**1** and [^{18}F]**2** were measured and expressed as log P values

of 2.00 ± 0.01 and 2.11 ± 0.01, respectively. As predicted, lipophilicity of [^{18}F]**2** was higher

than that of [^{18}F]**1**, due to the presence of two methyl groups at C2 and C6 positions.

Sulforhodamine B (SRB) assay

Cytotoxicity of HC derivatives was measured by carrying out the SRB assay for two cell

lines, human umbilical vascular endothelial cells (HUVEC) and rat C6 glioma cells, 72 h

after treatment with the compounds (Table 1). All of the compounds showed a similar trend

in cytotoxicity for the cell lines studied. HC had superior cytotoxicity to the other compounds

including curcumin, which was consistent with results in the literature for bovine aortic

endothelial cells.[12] The HC derivatives substituted with a mini-PEG moiety (**1** and **2**) showed

8

more potent cytotoxicity than the other HC derivatives against both HUVECs and C6 glioma

cells, and furthermore, 2,6-dimethyl derivative (**2**) was more potent than the corresponding

2,6-unsubstituted derivative (**1**). Thus, the two compounds, **1** and **2**, were selected for [18]F-

labeling.

Reduction with alcohol dehydrogenase

Reduction of **1** and **2** was performed using alcohol dehydrogenase, an enzyme known to be

involved in the reductive metabolism of curcumin.[26,27] Compound **1** was eluted at the

retention time between 37.9 and 38.9 min (Fig. 2A) and remained intact under complete

incubation conditions in the presence of alcohol dehydrogenase and NADPH (Fig. 2B). The

peak from 33.0 to 33.8 min was identified as an impurity derived from alcohol

dehydrogenase, which was also present in incubation of the enzyme itself (Fig. 2C).

Compound **2** was eluted at the retention time between 40.4 and 41.6 min (Fig. 2D) and

remained intact under complete incubation conditions (Fig. 2D and E). Both compounds were

also unchanged under conditions omitting NADPH (Fig. 2F). On the other hand, curcumin

was mostly converted to tetrahydrocurcumin (Fig. 2G and H), which was confirmed by the

same retention time as the authentic tetrahydrocurcumin (Fig. 2I).[17]

In vivo **metabolism studies in ICR mice**

HPLC chromatograms of the blood and liver samples obtained from mice injected with [^{18}F]**1** and [^{18}F]**2** showed the same pattern of radiometabolite formation (Fig. 3). Radioligand [^{18}F]**2** was metabolically more stable than [^{18}F]**1** in blood 5 min after injection, probably due to its higher lipophilicity (Fig. 3a). However, the two radioligands were below detection limit at 30 min except a polar peak at 4.8 min. This rapid metabolism were similar to that of curcumin.[28] On the other hand, two radiometabolites were detected in the liver samples of [^{18}F]**1** and [^{18}F]**2** 5 and 30 min after injection (Fig. 3c and d), and there were no radiometabolites detected at 60 min (data not shown). In order to identify whether one of the radiometabolites is a glucuronide conjugate, the 5-min liver samples of [^{18}F]**1** were incubated with β-glucuronidase. The results demonstrated that the radiometabolite, m1 (t_R = 24.2 min), was hydrolyzed to [^{18}F]**1** (t_R = 40.1 min) (Fig 3A-e), suggesting that m1 is [^{18}F]**1**-glucuronide. Based on the HPLC data of the known metabolites of curcumin, it is likely that m2 is its sulfate conjugate.[28]

Cellular uptake

We carried out the cellular uptake studies of [^{18}F]**1** and [^{18}F]**2** using two different cell lines, HUVECs and C6 glioma cells. HUVEC uptake of [^{18}F]**1** increased in a time-dependent

manner from 100% (2.2% ID) at 5 min to 160% (3.5% ID) at 120 min (P <0.01). Blocking

studies demonstrated inhibition of radioligand uptake in the presence of **1**, curcumin, and HC

by 56%, 64%, and 55%, respectively (P <0.001) (Fig. 4A and B). Similar results were

obtained using C6 cells; uptake increased from 100% (2.8% ID) at 5 min to 163% (4.6% ID)

at 120 min (P <0.01) and radioligand uptake was reduced in the presence of **1**, curcumin, and

HC by 52%, 52%, and 52%, respectively (P <0.001) (Fig. 4C and D).

HUVEC uptake of [^{18}F]**2** increased in a time-dependent manner from 100% (2.6% ID) at 5

min to 165% (4.2% ID) at 120 min (P <0.001). Blocking studies showed reduction of the

radioligand uptake in the presence of **2**, curcumin, and HC by 60%, 58%, and 58%,

respectively (P <0.001) (Fig. 4E and F). Similar results were obtained using C6 cells; uptake

from 100% (3.2% ID) at 5 min to 153% (4.9% ID) at 120 min (P <0.01) and reduction of the

radioligand uptake in the presence of **2**, curcumin, and HC by 61%, 52%, and 49%,

respectively (P <0.001) (Fig. 4G and H).

MicroPET imaging

MicroPET images of C6 glioma xenografted mice were acquired after injection with [^{18}F]**1**

and [^{18}F]**2** dissolved in 0.2% polysorbate 80 in saline, which is a FDA-approved inactive

ingredient and is compatible for clinical use. The images revealed accumulation of high

levels of radioactivity in the intestines at 30 min post-injection with slow clearance over time.

Tumor was not clearly detected in mice injected with [^{18}F]**1** (Fig. 5A), whereas it was clearly

detected at 30 min after injection of [^{18}F]**2** and uptake was retained at 60 min (Fig. 5B).

Region of interest (ROI) analysis of tumors in mice injected with [^{18}F]**1** revealed 1.10 ±

0.10% ID/g at 30 min and 0.97 ± 0.12% ID/g at 60 min. In contrast, significantly higher ROI

values were obtained in tumors of mice injected with [^{18}F]**2**: 3.30 ± 0.07% ID/g at 30 min (P

< 0.01) and 3.90 ± 0.70% ID/g at 60 min (P < 0.001) (Fig. 5C). Tumor to muscle uptake

ratios of [^{18}F]**1** and [^{18}F]**2** were 1.46 and 2.02 at 30 min and 1.28 and 2.28 at 60 min,

respectively.

Biodistribution

Biodistribution studies carried out immediately after microPET imaging of tumor-bearing

mice demonstrated accumulation of high levels of radioactivity in the intestines. Low levels

of femur uptake by both [^{18}F]**1** and [^{18}F]**2** indicated that the radioligands do not undergo *in*

vivo defluorination. Tumor uptake of [^{18}F]**1** at 65 min after injection was 0.98 ± 0.31% ID/g,

whereas that of [^{18}F]**2** was 3.20 ± 0.35% ID/g (Fig. 6). Although tumor uptake of [^{18}F]**2** was

significantly higher than that of [^{18}F]**1** (P < 0.01), tumor-to-background uptake ratios of the

two radioligands were within the same range (tumor/muscle and tumor/blood: 2.30 and 0.87

vs. 2.21 and 0.86, respectively). However, it is interesting to note that small intestine uptake was markedly higher for $[^{18}F]$**1** than for $[^{18}F]$**2** ($P < 0.05$) (Fig. 6).

Discussion

A few radiolabeled curcumin and hydrazinocurcumin derivatives have been developed to date for β-amyloid plaque imaging. Among these radioligands, ^{nat}Ga-labeled homodimers of curcumin derivatives were tested for cancer cellular uptake using their intrinsic fluorescence. However, none of these radioligands have been studied for tumor imaging. Our study as well as other reported studies showed that HC has more potent cytotoxicity than curcumin for various cancer cell lines (Table 1).[11] Furthermore, 2,6-dimethylcurcumin was shown to undergo significantly diminished reductive metabolism on olefinic double bonds compared with curcumin, possibly by creating steric hindrance against reductive metabolizing enzymes.[17] In this study, therefore, fluorine-substituted HC derivatives (**1**, **3**, and **5**) and their 2,6-dimethyl substituted compounds (**2**, **4**, and **6**) were synthesized. In compounds **1** and **2**, mini-polyethylene glycol (PEG) moiety was added between 4'-OH group of HC backbone and ^{18}F to improve their *in vivo* properties. ^{18}F-PEG has been successfully used to adjust lipophilicity of compounds while retaining their biological activity, as shown in the studies of ^{18}F-PEG-stilbene and styrylpyridines for β-amyloid plaque imaging.[29,30]

As HC is known to have inhibitory activity on endothelial cell proliferation,[12] cytotoxicity

of HC derivatives was measured for HUVECs in addition to C6 glioma cells using the SRB

assay (Table 1). Compounds **1** and **2** were selected for ^{18}F-labeling because of their potent

cytotoxicity against the two cells studied. Synthesis of radioligands ([^{18}F]**1** and [^{18}F]**2**) was

carried out by labeling bis-MOM protected precursors (**26** and **27**) with ^{18}F, followed by

deprotecting MOM groups. Attempts to prepare [^{18}F]**1** by [^{18}F]fluorination of unprotected or

4'-MOM protected tosylate precursor yielded the product in very low yield (< 3% based on

radio-TLC). Therefore, aromatic OH and pyrazole NH groups of **22** and **23** were selectively

protected with MOM groups in the presence of catalytic amounts of Adogen 464[®],[31,32] and

the residual aliphatic OH group was subsequently converted into tosylate ester. The bis-

MOM protected precursors were then used for the one-pot synthesis of radioligands in

relatively high yields and with high specific activity.

Metabolism of HC derivatives was assessed *in vitro* and *in vivo* to determine whether

dimethyl substitution on HC could prevent reduction of olefinic double bonds. *In vitro*

reductive metabolism study of **1** and **2** using alcohol dehydrogenase demonstrated that the

olefinic double bonds of **1** as well as **2** were not reduced, unlike curcumin.[26,27,33] In accord

with these results, attempts to synthesize tetrahydro- and hexahydro-forms of compounds **1**

and **2** using a previously reported method were not successful, whereas tetrahydro- and

hexahydro-curcumin, which are metabolite standards of curcumin, were readily synthesized using the same method.[26,33] *In vivo* metabolism study was performed using the blood and liver samples obtained from mice injected with the radioligands, because a host of endogenous molecules would be also detected by HPLC with UV absorption at 280 nm if non-radioactive compounds **1** and **2** were used instead of radiologands.[28] HPLC chromatograms of the liver samples showed that [^{18}F]**1** and [^{18}F]**2** were mostly biotransformed to two radiometabolites, both of which are most likely to be the conjugation products of the radioligands (Fig. 3). This result was consistent with that obtained from *in vitro* reduction of **1** and **2** with alcohol dehydrogenase (Fig. 2), suggesting that the pyrazole ring of HC derivatives is responsible for resistance to reductive metabolism because curcumin is known to be a substrate for reductive metabolism.[28,34]

It was reported that HC has inhibitory activity on endothelial cell proliferation and high antiangiogenesis activity,[12,13] and furthermore, compounds **1** and **2** showed cytotoxicity comparable to HC for HUVECs (Table 1). Therefore, we carried out the cellular uptake studies of [^{18}F]**1** and [^{18}F]**2** using two different cell lines, HUVECs and C6 glioma cells. Blocking studies were carried out using non-radioactive compound (**1** or **2**), curcumin, and HC. The results demonstrate that cellular uptake of [^{18}F]**2** is slightly higher than that of [^{18}F]**1**, probably because of the presence of two methyl groups in [^{18}F]**2**, which confer higher

15

lipophilicity than [18F]**1**. Similar levels of blocking of radioligand uptake by non-radioactive compounds, curcumin, and HC were obtained, suggesting that the radioligands may share the same binding sites as HC and curcumin.

MicroPET images acquired in C6 glioma xenografted mice after injection with radioligands revealed significantly higher radioactivity in the tumor of mice injected with [18F]**2** than with [18F]**1** (Fig. 5). However, the two radioligands showed similar tumor-to-background uptake ratios, except for the predominantly higher uptake of [18F]**1** by the small intestines, indicating its more rapid clearance. Furthermore, the high levels of radioactivity in the intestines of the two radioligands are similar to the known distribution of curcumin in rodents.[5] These results suggest that the differences in the *in vivo* uptake may be attributable to the higher lipophilicity of [18F]**2** than [18F]**1**.

It has been shown that HC has diverse biological activity probably resulting from its interaction with multiple targets.[7-14] Our microPET and biodistribution studies demonstrated high retention of radioactivity in tumors of C6 tumor-bearing mice. However, the molecular targets of these radioligands for the tumor uptake have not been identified. Therefore, further investigation may be necessary, not only to enhance the tumor-to-background uptake ratios of these radioligands through structural modifications, but also to elucidate their specific molecular targets.

16

Conclusion

Of six fluorine-substituted HC derivatives, compounds **1** and **2** were selected for ^{18}F-labeling

because of their potent cytotoxicity. Although *in vitro* cellular uptake of [^{18}F]**1** and [^{18}F]**2** was

comparable, *in vivo* properties of the radioligands in C6 glioma xenografted mice differed,

such that [^{18}F]**2** had significantly lower small intestine uptake than [^{18}F]**1** but higher uptake in

tumors and in other major organs, resulting in similar tumor to muscle and tumor to blood

uptake ratios. Furthermore, [^{18}F]**1** and [^{18}F]**2** were resistant to reductive metabolism *in vitro*

and *in vivo*, probably because of the presence of a pyrazole ring. To the best of our

knowledge, these are the first microPET studies of radiolabeled HC derivatives in tumor

xenografted mice.

Experimental

Materials and equipment

Chemicals, sulforhodamine-B, equine alcohol dehydrogenase, β-glucuronidase, and

polysorbate 80 (10% in water) were purchased from Sigma-Aldrich (St. Louis, MO, USA).

^{1}H NMR spectra were obtained using a Bruker Avance 500 (500 MHz) spectrometer

(Rheinstetten, Germany), and chemical shifts (δ) were reported as the ppm downfield of the

internal tetramethylsilane. All NMR samples were prepared in CDCl$_3$ or DMSO-d_6 at 20 mM,

and under these conditions, the NH and OH protons were not detected in all compounds. ^{13}C

NMR spectra were obtained on a Bruker Avance 600 (150 MHz) spectrometer. Two-

dimensional ROESY experiments were carried out on a Bruker Avance 600 (600 MHz)

spectrometer at National Center for Inter-University Research Facilities, Seoul National

University (Seoul, Korea). The spectra were acquired using the states-TPPI mode with

mixing times of 700 ms and acquisition times of 0.14 s. Electron impact (EI) and fast atom

bombardment (FAB) mass spectra were obtained using a JMS-700 Mstation (JEOL Ltd,

Tokyo, Japan). Purification and analysis of radioligands were performed using HPLC

(Thermo Scientific, Waltham, MA, USA) equipped with a semi-preparative column (YMC-

Pack Si, 5 μm, 10 × 250 mm) or an analytical column (YMC-Pack C18, 5 μm, 4.6 × 250

mm). The eluent was monitored simultaneously, using UV (254 nm) and NaI(T1)

radioactivity detectors. TLC was performed on Merck F$_{254}$ silica plates and analyzed on a

Bioscan radio-TLC scanner (Washington, D.C., USA).

[^{18}F]Fluoride was produced by the ^{18}O(p,n)^{18}F reaction using a GE Healthcare PETtrace

cyclotron (Uppsala, Sweden). Radioactivity was measured in a dose calibrator (Biodex

Medical Systems, Shirley, NY, USA) and tissue radioactivity was measured in a Wizard^2

automatic gamma counter (PerkinElmer, Waltham, MA, USA). MicroPET images were

acquired at the Center for Molecular and Cellular Imaging, Samsung Biomedical Research

Institute (SBRI, Seoul, Korea) using an Inveon microPET/CT scanner (Siemens Medical

Solutions, Malvern, PA, USA).

Synthesis of fluorine-substituted HC derivatives (1, 3, and 5)

Hydrazine hydrate (3 eq) and catalytic amounts of acetic acid (0.5 eq) were added to a

solution of compound **7** (50 mg, 0.10 mmol), **9** (50 mg, 0.11 mmol), or **11** (50 mg, 0.12

mmol) in ethanol (500 μL), and the reaction solution was heated at 80 ^{o}C for 18 h. At the end

of the reaction, the reaction mixture was extracted twice with ethyl acetate (30 mL × 2), and

the organic layer was washed with a saturated $NaHCO_3$ solution and with brine, and then

dried over Na_2SO_4. The product was purified using flash column chromatography (1:2

hexane-ethyl acetate) to yield **1** (26.8 mg, 53%), **3** (20.3 mg, 45%), or **5** (37.6 mg, 74%) as a

light yellow solid.

1: Purity (HPLC), 99.0%; ^{1}H NMR (CDCl$_3$) δ 3.84 (dt, J = 26.5 and 4.0 Hz, 2H), 3.88(s, 3H),

3.91 (s, 3H), 3.94 (t, J = 5.0 Hz, 2H), 4.23 (t, J = 5.0 Hz, 2H), 4.59 (dt, J = 47.5 and 4.0 Hz,

2H), 6.59 (s, 1H), 6.90 (d, J = 14.0 Hz, 4H), 6.93 (d, J = 4.0 Hz, 4H), 6.97-6.98 (m, 2H); ^{13}C

NMR (CDCl$_3$) δ 149.49, 147.52, 146.82, 145.82, 144.53, 135.29, 131.26, 129.80, 121.66,

114.60, 113.59, 112.23, 110.98, 109.19, 108.10, 101.07, 83.20 (d, J = 169.1 Hz), 70.65 (d, J =

19.4 Hz), 69.90, 68.74, 55.88, 55.85; MS (FAB) *m/z* 455 (M$^+$ + H); HRMS calcd for

C$_{25}$H$_{28}$FN$_2$O$_5$, 455.1982; found, 455.1990.

3: Purity (HPLC), 99.0%; ^{1}H NMR (CDCl$_3$) δ 3.89 (s, 3H), 3.90 (s, 3H), 4.30 (dt, *J* = 23.0

and 4.0 Hz, 2H), 4.80 (dt, *J* = 46.0 and 4.5 Hz, 2H), 6.60 (s, 1H), 6.88 (d, *J* = 9.5 Hz, 2H),

6.93-6.97 (m, 6H), 6.99 (d, *J* = 15.5 Hz, 2H); ^{13}C NMR (CDCl$_3$) δ 149.28, 147.48, 146.82,

145.81, 144.50, 134.21, 130.88, 129.80, 122.85, 114.18, 113.02, 112.21, 109.97, 108.99,

108.23, 99.84, 82.80 (d, *J* = 169.0 Hz), 70.38 (d, *J* = 19.4 Hz), 55.88, 55.83; MS (FAB) *m/z*

411 (M$^+$ + H); HRMS calcd for C$_{23}$H$_{24}$FN$_2$O$_4$, 411.1720; found, 411.1728.

5: Purity (HPLC), 99.8%; ^{1}H NMR (CDCl$_3$) δ 2.25 (dt, *J* = 26.5 and 6.0 Hz, 2H), 3.92 (s, 3H),

3.95 (s, 3H), 4.20 (q, *J* = 5.0 Hz, 2H), 4.70 (dt, J = 47.0 and 6.0 Hz, 2H), 6.16 (s, 1H), 6.89-

6.95 (m, 5H), 7.00-7.07 (m, 5H); ^{13}C NMR (CDCl$_3$) δ 149.38, 147.51, 147.02, 146.03,

145.12, 135.36, 131.28, 130.01, 122.56, 115.90, 114.32, 112.78, 111.01, 109.84, 108.14,

101.03, 82.54 (d, *J* = 170.0 Hz), 70.54 (d, *J* = 18.8 Hz), 55.88, 55.84, 30.70; MS (FAB) *m/z*

425 (M$^+$ + H); HRMS calcd for C$_{24}$H$_{26}$FN$_2$O$_4$, 425.1877; found, 425.1875.

Synthesis of fluorine-substituted 2,6-dimethyl-HC derivatives (2, 4, and 6)

Compounds **2**, **4**, and **6** were synthesized as described for syntheses of **1**, **3**, and **5** using **8** (50

mg, 0.10 mmol), **10** (30 mg, 0.06 mmol), or **12** (50 mg, 0.10 mmol) instead of **7**, **9**, or **11**.

Flash column chromatography (hexane-ethyl acetate) yielded **2** (34.5 mg, 73%), **4** (26.4 mg, 89%), or **6** (34.6 mg, 58%) as a light yellow solid. Configurations of 2,6-dimethyl groups of **2** were determined by 2D ROESY.

2: Purity (HPLC), 99.6%; ^{1}H NMR (CDCl$_3$) δ 2.30 (s, 6H), 3.84 (dt, J = 30.5 and 4.0 Hz, 2H), 3.87(s, 3H), 3.91(s, 3H), 3.94 (t, J = 5.0 Hz, 2H), 4.23 (t, J = 4.5 Hz, 2H), 4.59 (dt, J = 47.5 and 4.0 Hz, 2H), 6.58 (s, 1H), 6.90 (d, J = 9.8 Hz, 2H), 6.92 (d, J = 9.5 Hz, 2H), 6.93 (d, J = 2.5 Hz, 2H), 6.98 (s,1H), 6.99 (s, 1H); ^{13}C NMR (CDCl$_3$) δ 149.09, 147.15, 146.25, 144.70, 130.79, 129.54, 126.74, 126.53, 122.55, 121.89, 114.27, 113.33, 112.98, 111.82, 99.37, 83.20 (d, J = 169.0 Hz), 70.61 (d, J = 19.6 Hz), 69.83, 68.57, 55.86, 55.84, 16.07; MS (FAB) m/z 483 (M$^+$ + H); HRMS calcd for C$_{27}$H$_{32}$FN$_2$O$_5$, 483.2295; found, 483.2290.

4: Purity (HPLC), 98.9%; ^{1}H NMR (CDCl$_3$) δ 2.28 (s, 6H), 3.88 (s, 3H), 3.91 (s, 3H), 4.32 (dt, J = 36.5 and 4.5 Hz, 2H), 4.79 (dt, J = 47.0 and 4.5 Hz, 2H), 6.59 (s, 1H), 6.88 (s, 1H), 6.91-6.94 (m, 5H), 6.98 (s, 1H), 7.00(s, 1H); ^{13}C NMR (CDCl$_3$) δ 149.28, 146.83, 146.22, 144.71, 131.28, 129.52, 126.77, 126.43, 122.59, 121.86, 114.26, 113.77, 113.15, 111.77, 99.44, 81.96 (d, J = 170.5 Hz), 68.42 (d, J = 19.6 Hz), 55.95, 55.87, 16.03; MS (FAB) m/z 439 (M$^+$ + H); HRMS calcd for C$_{25}$H$_{28}$FN$_2$O$_4$, 439.2033; found, 439.2025.

6: Purity (HPLC), 100%; ^{1}H NMR (CDCl$_3$) δ 2.24 (dt, J = 26.5 and 6.0 Hz, 2H), 2.29 (s, 3H), 2.30 (s, 3H), 3.88 (s, 3H), 3.91 (s, 3H), 4.18 (q, J = 6.0 Hz, 2H), 4.68 (dt, J = 47.5 and 6.0 Hz,

2H), 6.59 (s, 1H), 6.90 (d, $J = 9.8$ Hz, 2H), 6.94 (d, $J = 4.0$ Hz, 4H), 6.97 (s,1H), 6.98 (s, 1H);

^{13}C NMR (CDCl$_3$) δ 149.33, 146.89, 146.20, 144.75, 131.22, 129.48, 127.01, 126.68, 122.63,

121.88, 114.24, 113.82, 113.18, 111.74, 99.47, 81.95 (d, $J = 170.7$ Hz), 68.43 (d, $J = 20.6$ Hz),

55.99, 55.90, 31.9, 16.02; MS (FAB) m/z 453 (M$^+$ + H); HRMS calcd for C$_{26}$H$_{30}$FN$_2$O$_4$,

453.2190; found, 453.2191.

Synthesis of fluorine-substituted curcumin derivatives (7, 9, and 11)

B$_2$O$_3$ (0.22 mmol) was added to a solution of **13** (50 mg, 0.21 mmol) in ethyl acetate and the

reaction solution was heated at 80 ^{o}C for 30 min. The reaction mixture was then reacted with

an ethyl acetate solution (700 μL) of **17**, **18**, or **19** (0.21 mmol) and (n-BuO)$_3$B (0.22 mmol).

After stirring at 80 ^{o}C for 30 min, piperidine (14.1 μL, 0.14 mmol) was added dropwise to the

mixture, which was then stirred at 100 ^{o}C for 2 h. The solution was cooled and treated with

0.4 N HCl (700 μL) at 50 ^{o}C for 30 min. The reaction mixture was extracted twice with ethyl

acetate (30 mL × 2), and the organic layer was washed with water and dried over Na$_2$SO$_4$.

The product was purified using flash column chromatography (hexane-ethyl acetate) to give **7**

(65.1 mg, 67%), **9** (33.1 mg, 38%), or **11** (54.5 mg, 61%) as a yellow solid.

7: ^{1}H NMR (CDCl$_3$) δ 3.76 (dt, $J = 31.5$ and 4.0 Hz, 2H), 3.80 (t, $J = 5.0$ Hz, 2H), 3.84 (s,

6H), 4.24 (t, $J = 4.5$ Hz, 2H), 4.58 (dt, $J = 48.5$ and 4.3 Hz, 2H), 6.09 (s, 1H), 6.76 (d, $J =$

16.0 Hz, 1H), 6.82 (d, J = 8.5 Hz, 1H), 6.83 (d, J = 15.5 Hz, 1H), 7.03 (d, J = 8.5 Hz, 1H),

7.24 (dd, J = 8.3 and 1.5 Hz, 1H), 7.32 (d, J = 2.0 Hz, 1H), 7.35 (d, J = 1.5 Hz, 2H), 7.56 (d,

J = 16.0 Hz, 1H), 7.58 (d, J = 16.0 Hz, 1H); MS (FAB) m/z 459 (M$^+$ + H); HRMS calcd for

$C_{25}H_{28}FO_7$, 459.1819; found, 459.1819.

9: ^{1}H NMR (CDCl$_3$) δ 3.93 (s, 3H), 3.95(s, 3H), 4.31 (dt, J =27.0 and 3.5Hz, 2H), 4.78 (dt, J

= 47.5 and 4.3 Hz, 2H), 5.86 (s, 1H), 6.48 (d, J = 16.0 Hz, 1H), 6.51 (d, J = 16.0 Hz, 1H),

6.92 (d, J = 8.5 Hz, 1H), 6.94 (d, J = 8.5 Hz, 1H), 7.05 (d, J = 1.5 Hz, 1H), 7.09 (d, J = 1.5

Hz, 1H), 7.13 (dd, J = 8.0 and 1.5 Hz, 2H), 7.60 (d, J = 16.0 Hz, 2H); MS (FAB) m/z 415 (M$^+$

+ H); HRMS calcd for $C_{23}H_{24}FO_6$, 415.1557; found, 415.1557.

11: ^{1}H NMR (CDCl$_3$) δ 2.22-2.33 (m, 2H), 3.91 (s, 3H), 3.94 (s, 3H), 4.20 (t, J = 6.0 Hz, 2H),

4.62 (t, J = 6.0 Hz, 1H), 4.72 (t, J = 5.5 Hz, 1H), 5.81 (s, 1H), 6.47 (dd, J = 15.5 and 7.8 Hz,

2H), 6.93 (dd, J = 20.0 and 9.9 Hz, 2H), 7.02-7.12 (m, 4H), 7.59 (d, J = 15.5 Hz, 2H); MS

(EI) m/z 428 (M$^+$); HRMS calcd for $C_{24}H_{25}FO_6$, 428.1635; found, 428.1638. ^{1}H NMR data

agreed with literature values.[6]

Synthesis of fluorine-substituted 2,6-dimethyl-curcumin derivatives (8, 10, and 12)

Compounds **8**, **10**, and **12** were synthesized as described for syntheses of **7**, **9**, and **11** using

14 (100.0 mg, 0.38 mmol) instead of **13**. Flash column chromatography (hexane-ethyl

acetate) gave **8** (143.2 mg, 78%), **10** (65.8 mg, 39%), or **12** (60.0 mg, 37%) as a light yellow

solid.

8: ^{1}H NMR (DMSO-d_6) δ 2.15 (s, 6H), 3.76 (dt, J = 31.5 and 3.5 Hz, 2H), 3.78(t, J = 3.5 Hz, 2H), 3.79 (s, 3H), 3.81 (s, 3H), 4.15 (t, J = 4.5 Hz, 2H), 4.60 (dt, J = 47.5 and 4.0 Hz, 2H), 6.61 (s, 1H), 6.86 (d, J = 8.5 Hz, 1H), 7.06 (d, J = 8.5 Hz, 2H), 7.11-7.15 (m, 3H), 7.62 (s, 1H), 7.63 (s, 1H); MS (FAB) m/z 487 (M[+] + H); HRMS calcd for $C_{27}H_{32}FO_7$, 487.2132; found, 487.2130.

10: ^{1}H NMR (CDCl$_3$) δ 2.29 (s, 6H), 3.93 (s, 3H), 3.97 (s, 3H), 4.31 (dt, J = 25.0 and 3.0 Hz, 2H), 4.80 (dt, J = 47.5 and 4.0 Hz, 2H), 6.31 (s, 1H), 6.94 (d, J = 7.0, 2H), 6.97 (d, J = 7.0, 2H), 7.02 (d, J = 6.5, 2H), 7.55 (s, 2H); MS (FAB) m/z 443 (M[+] + H); HRMS calcd for $C_{25}H_{28}FO_7$, 443.1870; found, 443.1864.

12: ^{1}H NMR (CDCl$_3$) δ 2.18 (s, 6H), 2.24 (dt, J = 26.5 and 6.0 Hz, 2H), 3.89 (s, 3H), 3.92 (s, 3H), 4.20 (t, J = 6.5 Hz, 2H), 4.68 (dt, J = 47.0 and 6.0 Hz, 2H), 6.30 (s, 1H), 6.92-7.03 (m, 6H), 7.54 (s, 2H); MS (EI) m/z 456 (M[+]); HRMS calcd for $C_{26}H_{29}FO_6$, 456.1948; found, 456.1946.

Synthesis of 5-hydroxy-1-(4-hydroxy-3-methoxyphenyl)-hexa-1,4-dien-3-one and its dimethyl-substituted derivative (13 and 14)

B$_2$O$_3$ (733.8 mg, 10.54 mmol) was added to a solution of 2,4-pentanedione (600.7 mg, 6.00

mmol) in ethyl acetate, and the solution was stirred at 80 $^\circ$C for 30 min. An ethyl acetate

solution (2.7 mL) of vanillin (912.2 mg, 6.00 mmol) and (*n*-BuO)$_3$B (0.46 mL, 1.70 mmol)

was added to the reaction mixture. After stirring at 80 $^\circ$C for 30 min, *n*-BuNH$_2$ (0.23 mL,

2.28 mmol) was added dropwise to the mixture, which was then stirred at 80 $^\circ$C for 1 h. The

solution was cooled and treated with 1 N HCl (4.5 mL) at 50 $^\circ$C for 30 min. The reaction

mixture was extracted twice with ethyl acetate (200 mL × 2), and the organic layer was

washed with water and dried over Na$_2$SO$_4$. Flash column chromatography followed by

recrystallization from ethanol gave **13** (600 mg, 43%) as a yellow solid. Compound **14** was

synthesized as described for synthesis of **13** using 3,5-heptanedione. Flash column

chromatography (3:1 hexane-ethyl acetate) yielded **14** (516.9 mg, 33%) as a yellow solid.

13: ^{1}H NMR (CDCl$_3$) δ 2.15 (s, 3H), 3.94 (s, 3H), 5.84 (s, 1H), 6.32 (d, *J* = 16.0 Hz, 1H),

6.93 (d, *J* = 15.5 Hz, 1H), 7.09 (d, *J* = 10.5 Hz, 2H), 7.53 (d, *J* = 16.0 Hz, 1H); MS (EI) *m/z*

234 (M$^+$); HRMS calcd for C$_{13}$H$_{14}$O$_4$, 234.0892; found, 234.0891.

14: ^{1}H NMR (CDCl$_3$) δ 1.19 (t, *J* = 7.5 Hz, 3H), 2.10 (s, 3H), 2.44 (q, *J* = 7.5 Hz, 2H), 3.91 (s,

3H), 5.87 (s, 1H), 6.91 (d, *J* = 1.5 Hz, 1H), 6.90-6.97 (m, 2H), 7.50 (s, 1H); MS (EI) *m/z* 262

(M$^+$); HRMS calcd for C$_{15}$H$_{18}$O$_4$, 262.1205; found,262.1206.

Synthesis of 4-(2-(2-fluoroethoxy)ethoxy)-3-methoxybenzaldehyde (17)

2-(2-Chloroethoxy)ethanol (1.0 mL, 9.85 mmol) was added to a solution of vanillin (1 g, 6.57 mmol) in DMF (100 mL) in the presence of K_2CO_3 (1.18 g, 8.54 mmol), and the reaction mixture was stirred at 100 ^{o}C for 5 h. At the end of the reaction, the mixture was diluted with water, extracted twice with CH_2Cl_2 (150 mL × 2), and the combined organic layer was washed with water (50 mL) and with a saturated ammonium chloride solution to remove residual DMF and dried over Na_2SO_4. Flash column chromatography (1:5 hexane-ethyl acetate) yielded **15** (986.3 mg, 63%) as a white solid.

15: ^{1}H NMR ($CDCl_3$) δ 3.69 (t, J = 4.4 Hz, 2H), 3.77 (t, J = 5.0 Hz, 2H), 3.94 (s, 3H), 3.96 (t, J = 4.5 Hz, 2H), 4.26 (t, J = 4.6 Hz, 2H), 6.98 (d, J = 7.9 Hz, 1H), 7.39-7.45 (m, 2H), 9.85 (s, 1H); MS (EI) m/z 240 (M$^+$); HRMS calcd for $C_{12}H_{16}O$, 240.0998; found, 240.0996.

Compound **15** (500 mg, 2.08 mmol) was dissolved in CH_2Cl_2, and Et_3N (1.74 mL, 12.48 mmol) was added. The mixture was stirred at room temperature for 1 h, and then methanesulfonyl chloride (193.3 mg, 2.49 mmol) was added at 0 ^{o}C, and the mixture was stirred at room temperature for 6 h. The reaction was quenched by addition of a saturated ammonium chloride solution (50 mL). The reaction mixture was extracted twice with CH_2Cl_2 (50 mL × 2), and the combined organic layer was washed with water (50 mL) and dried over Na_2SO_4. Flash column chromatography (25:1 CH_2Cl_2-methanol) gave **16** (632 mg, 95%) as a white solid.

16 : ^{1}H NMR (CDCl$_3$) δ 3.05 (s, 3H), 3.86 (t, J = 3.0 Hz, 2H), 3.91 (s, 3H), 3.95 (t, J = 5.0 Hz,

2H), 4.27 (t, J = 4.5 Hz, 2H), 4.41 (t, J = 4.0 Hz, 2H), 6.99 (d, J = 8.0 Hz, 1H), 7.41-7.45 (m,

2H), 9.86 (s, 1H); MS (EI) m/z 318 (M$^+$); HRMS calcd for C$_{13}$H$_{18}$O$_7$S, 318.0773; found,

318.0796.

Compound **16** (500 mg, 1.57 mmol) and cesium fluoride (715 mg, 4.71 mmol) were

dissolved in t-BuOH (20 mL), and the reaction mixture was stirred at 100 ^{o}C for 19 h. At the

end of the reaction, the mixture was diluted with water, extracted twice with ethyl acetate

(100 mL × 2), and the combined organic layer was washed with water (100 mL) and dried

over Na$_2$SO$_4$. Flash column chromatography (1:1 hexane-ethyl acetate) yielded **17** (323.8 mg,

85%) as a white solid.

17: ^{1}H NMR (CDCl$_3$) δ 3.84 (dt, J = 25.5 and 5Hz, 2H), 3.92 (s, 3H), 3.97 (t, J = 5.0 Hz, 2H),

4.29 (t, J = 4.5 Hz, 2H), 4.58 (dt, J = 47.5 and 4.5 Hz, 2H), 7.01 (d, J = 7.5 Hz, 1H), 7.41 (d,

J = 2.0 Hz, 1H), 7.01 (dd, J = 8.5 and 1.5 Hz, 1H), 9,86 (s, 1H); MS (EI) m/z 242 (M$^+$);

HRMS calcd for C$_{12}$H$_{15}$FO$_4$, 242.0954; found, 242.0956.

Synthesis of 4-(2-fluoroethoxy)-3-methoxybenzaldehyde (18) and 4-(3-fluoropropoxy)-3-

methoxy benzaldehyde (19)

2-Fluoroethyl or 3-fluoropropyl tosylate (4.27 mmol) was added to a solution of vanillin (500

mg, 3.28 mmol) in CH_3CN (50 mL) in the presence of K_2CO_3 (590 mg, 4.27 mmol), and the

reaction mixture was stirred at 110 °C for 3 h. At the end of the reaction, the mixture was

diluted with water, extracted with ethyl acetate (100 mL), and the combined organic layer

was washed with water (100 mL) and dried over Na_2SO_4. Flash column chromatography

(hexane-ethyl acetate) afforded **18** (428.2 mg, 67%) or **19** (595.5 mg, 86%) as a white solid.

18: ^1H NMR ($CDCl_3$) δ 3.94 (s, 3H), 4.36 (dt, $J = 27.0$ and 4.5 Hz, 2H), 4.82 (dt, $J = 47.5$ and

4.0 Hz, 2H), 7.00 (d, $J = 8.0$ Hz, 1H), 7.43 (d, $J = 1.5$ Hz, 1H), 7.45 (dd, $J = 8.3$ and 2.0 Hz,

1H), 9,87 (s, 1H); MS (EI) m/z 198 (M^+); HRMS calcd for $C_{10}H_{11}FO_3$, 198.0692; found,

198.0694.

19: ^1H NMR ($CDCl_3$) δ 2.26 (dt, $J = 26.5$ and 5.5 Hz, 2H), 3.93 (s, 3H), 4.23-4.26 (m, 2H),

4.68 (dt, $J = 47.0$ and 6.0 Hz, 2H), 7.00 (d, $J = 8.5$ Hz, 1H), 7.42 (d, $J = 1.5$ Hz, 1H), 7.45 (dd,

$J = 8.5$ and 2.0 Hz, 1H), 9.86 (s, 1H); MS (EI) m/z 212 (M^+); HRMS calcd for $C_{11}H_{13}FO_3$,

212.0849; found, 212.0845.

Synthesis of curcumin derivatives (20 and 21)

B_2O_3 (128.10 mg, 1.84 mmol) was added to a solution of **13** or **14** (1.84 mmol) in ethyl

acetate (2 mL), and stirred at 80 °C for 30 min. An ethyl acetate solution (2 mL) of **15** (300

mg, 1.53 mmol) and (n-BuO)$_3$B (453 μL, 1.68 mmol) was added to the reaction mixture.

After stirring at 80 °C for 30 min, piperidine (75 μL, 0.76 mmol) was added to the mixture, which was then stirred at 80 °C for 1 h. The solution was cooled and treated with 0.4 N HCl (2 mL) at 50 °C for 30 min. The reaction mixture was extracted twice with ethyl acetate (100 mL × 2), and the combined organic layer was washed with water (100 mL) and dried over Na_2SO_4. Flash column chromatography followed by recrystallization from acetone gave **20** (238.5 mg, 34%) or **21** (317.2 mg, 42%) as a yellow solid.

20: ^{1}H NMR (CDCl$_3$) δ 3.69 (t, J = 4.0 Hz, 2H), 3.77 (t, J = 3.0 Hz, 2H), 3.92 (s, 3H), 3.93 (t, J = 4.0 Hz, 2H), 3.95 (s, 3H), 4.22 (t, J = 4.5 Hz, 2H), 6.30 (s, 1H), 6.47 (d, J = 16.0 Hz, 1H), 6.49 (d, J = 15.5 Hz, 1H), 6.90 (d, J = 8.5 Hz, 1H), 6.93 (d, J = 8.0 Hz, 1H), 7.05 (d, J = 2.0 Hz, 1H), 7.08 (d, J = 1.5 Hz, 1H), 7.12 (d, J = 8.5 Hz, 2H), 7.59 (d, J = 16.0 Hz, 2H); MS (FAB) m/z 457 (M$^+$ + H); HRMS calcd for $C_{25}H_{29}O_8$, 457.1862; found, 457.1868.

21: ^{1}H NMR (CDCl$_3$) δ 2.18 (s, 6H), 3.69 (t, J = 4.5 Hz, 2H), 3.77 (t, J = 4.5 Hz, 2H), 3.89 (s, 3H), 3.92 (s, 3H), 3.93 (t, J = 5.0 Hz, 2H), 4.23 (t, J = 4.5 Hz, 2H), 6.30 (s, 1H), 6.94 (d, J = 9.0 Hz, 1H), 6.95 (d, J = 2.0 Hz, 1H), 6.96 (d, J = 9.5 Hz, 1H), 6.97 (d, J = 1.5 Hz, 1H), 7.02 (d, J = 8.0 Hz, 2H), 7.54 (s, 2H); MS (FAB) m/z 485 (M$^+$ + H); HRMS calcd for $C_{27}H_{33}O_8$, 485.2175; found, 485.2173.

Synthesis of HC derivatives (22 and 23)

Hydrazine hydrate (30.95 μL, 0.99 mmol) and acetic acid (18.89 μL, 0.33 mmol) were added to a solution of **20** or **21** (0.33 mmol) in EtOH (3 mL), and the reaction mixture was stirred at 80 °C for 18 h. At the end of the reaction, the reaction mixture was extracted twice with ethyl acetate (30 mL × 2), and the organic layer was washed with a saturated $NaHCO_3$ solution and with brine and then dried over Na_2SO_4. Flash column chromatography (CH_2Cl_2-methanol) gave **22** (99.8 mg, 67%) or **23** (119.4 mg, 75%) as a light yellow solid.

22: ^{1}H NMR ($CDCl_3$) δ 3.70 (t, J = 4.5 Hz, 2H), 3.77 (t, J = 3.0 Hz, 2H), 3.89 (s, 3H), 3.92 (t, J = 4.5 Hz, 2H), 3.93 (s, 3H), 4.20 (t, J = 4.5 Hz, 2H), 6.59 (s, 1H), 6.87-6.91 (m, 5H), 7.01 (d, J = 4.5 Hz, 3H), 7.00-7.03 (m, 2H); MS (FAB) m/z 453 (M^+ + H); HRMS calcd for $C_{25}H_{29}N_2O_6$, 453.2026; found, 453.2015.

23: ^{1}H NMR ($CDCl_3$) δ 2.29 (s, 3H), 2.30 (s, 3H), 3.69 (t, J = 4.5 Hz, 2H), 3.77 (t, J = 3.5 Hz, 2H), 3.89 (s, 3H), 3.90 (t, J = 4.5 Hz, 2H), 3.91 (s, 3H), 4.18 (t, J = 6.3 Hz, 2H), 6.23 (s, 1H), 6.87-6.92 (m, 4H), 6.99 (d, J = 3.0 Hz, 2H), 7.01 (s, 1H), 7.03 (s, 1H); MS (FAB) m/z 481 (M^+ + H); HRMS calcd for $C_{27}H_{33}N_2O_6$, 481.2339; found, 481.2327.

Synthesis of bis-MOM-protected HC derivatives (24 and 25)

Chloromethyl methyl ether (45.6 μL, 0.60 mmol) was added to a solution of **22** or **23** (0.15 mmol) in CH_2Cl_2 (877 μL) in the presence of Adogen 464® (17.56 μL) and 2 N NaOH (293

μL), and the reaction mixture was stirred at room temperature for 20 min. At the end of the

reaction, the mixture was diluted with water and extracted with CH_2Cl_2 (20 mL), and the

organic layer was then dried over Na_2SO_4. Flash column chromatography (1:2 hexane-ethyl

acetate) yielded **24** (47.1 mg, 58%) or **25** (45.2 mg, 53%) as a yellow oil.

24: ^{1}H NMR ($CDCl_3$) δ 3.39 (s, 3H), 3.53 (s, 3H), 3.69 (t, $J = 3.0$ Hz, 2H), 3.78 (s, 3H), 3.85

(t, $J = 4.0$ Hz, 2H), 3.93 (s, 3H), 4.02 (t, $J = 6.0$ Hz, 2H), 4.27 (t, $J = 3.0$ Hz, 2H), 5.25 (s, 2H),

5.51 (s, 2H), 6.74 (s, 1H), 6.78 (d, $J = 8.5$ Hz, 1H), 6.90 (d, $J = 8.5$ Hz, 1H), 6.93-7.14 (m,

6H), 7.16-7.19 (m, 2H); MS (FAB) m/z 541 ($M^+ + H$); HRMS calcd for $C_{29}H_{37}N_2O_8$,

541.6168; found, 541.6169.

25: ^{1}H NMR ($CDCl_3$) δ 2.26 (s, 3H), 2.33 (s, 3H), 3.49 (s, 3H), 3.53 (s, 3H), 3.70 (t, $J = 3.0$

Hz, 2H), 3.77 (t, $J = 3.5$ Hz, 2H), 3.89-3.93 (m, 8H), 4.21 (t, $J = 3.0$ Hz, 2H), 5.25 (s, 2H),

5.45 (s, 2H), 6.49 (s, 1H), 6.83 (d, $J = 1.5$ Hz, 1H), 6.86 (d, $J = 1.2$ Hz, 1H), 6.90-6.96 (m,

4H), 7.08-7.16 (m, 2H); MS (FAB) m/z 569 ($M^+ + H$); HRMS calcd for $C_{31}H_{41}N_2O_8$,

569.2863; found, 569.2867.

Synthesis of precursors (26 and 27)

Et_3N (12.5 μL, 0.09 mmol) was added to a solution of **24** or **25** (0.06 mmol) in CH_2Cl_2 (500

μL), followed by addition of *p*-toluenesulfonyl chloride (13.3 mg, 0.07 mmol). The reaction

mixture was stirred at room temperature for 20 h. At the end of reaction, the mixture was

diluted with water (20 mL), extracted twice with CH_2Cl_2 (20 mL), and the organic layer was

dried over Na_2SO_4. Flash column chromatography (1:2 hexane-ethyl acetate) yielded **26** (31.0

mg, 73%) or **27** (36.6 mg, 83%) as a colorless viscous oil.

26: Purity (HPLC), 96.5%; ^{1}H NMR (CDCl$_3$) δ 2.31 (s, 3H), 3.47 (s, 3H), 3.49 (t, J = 3.5 Hz,

2H), 3.54 (s, 3H), 3.85 (t, J = 3.5 Hz, 2H), 3.90 (s, 3H), 3.91 (s, 3H), 4.26 (t, J = 4.5 Hz, 2H),

4.38 (t, J = 4.0 Hz, 2H), 5.25 (d, J = 3.5 Hz, 2H), 5.45 (s, 2H), 6.49 (s, 1H), 6.83 (dd, J = 10.0

and 2.5 Hz, 2H), 6.87-6.95 (m, 4H), 7.08 (d, J = 10.0 Hz, 1H), 7.16 (d, J = 8.5 Hz, 1H), 7.34

(d, J = 7.0 Hz, 2H), 7.82 (d, J = 8.0 Hz, 2H); ^{13}C NMR (CDCl$_3$) δ 149.85, 148.10, 147.12,

145.71, 132.78, 131.03, 128.99, 128.01, 126.91, 122.55, 121.89, 116.27, 113.43, 113.02,

112.87, 111.80, 111.61, 110.98, 101.03, 97.86, 96.61, 82.09, 71.85, 68.97, 68.44, 67.01, 56.80,

56.47, 56.11, 55.54, 23.01; MS (FAB) m/z 695 (M$^+$ + H); HRMS calcd for $C_{36}H_{43}N_2O_{10}S$,

695.2685; found, 695.2688.

27: Purity (HPLC), 99.0%; ^{1}H NMR (CDCl$_3$) δ 2.27 (s, 3H), 2.30 (s, 3H), 2.33 (s, 3H), 3.48

(s, 3H), 3.54 (s, 3H), 3.68 (t, J = 2.5 Hz, 2H), 3.77 (t, J = 3.5 Hz, 2H), 3.83 (t, J = 4.0 Hz, 2H),

3.89 (s, 3H), 3.91 (s, 3H), 4.26 (t, J = 3.0 Hz, 2H), 5.26 (s, 2H), 5.45 (s, 2H), 6.47 (s, 1H),

6.83 (d, J = 9.5, 1H), 6.87 (d, J = 8.5, 1H), 6.89-6.96 (m, 4H), 7.07 (d, J = 11.5 Hz, 1H), 7.16

(d, J = 8.0 Hz, 1H), 7.31 (d, J = 8.0 Hz, 2H)), 7.80 (d, J = 8.5 Hz, 2H); ^{13}C NMR (CDCl$_3$) δ

149.18, 147.26, 144.74, 132.02, 130.00, 129.89, 128.19, 126.73, 122.09, 116.12, 113.60,

113.49, 113.28, 113.14, 113.10, 112.99, 102.99, 96.75, 95.60, 80.05, 70.93, 69.83, 68.67,

66.99, 56.81, 56.42, 56.10, 55.41, 22.89, 15.91; MS (FAB) m/z 723 ($M^+ + H$); HRMS calcd

for $C_{38}H_{47}N_2O_{10}S$, 723.2951; found, 723.2946.

Radiochemical synthesis of [^{18}F]1 and [^{18}F]2

[^{18}F]Fluoride (185-1,110 MBq) was placed in a Vacutainer containing n-Bu$_4$NHCO$_3$. Three

azeotropic distillations were performed using 200- to 300-μL aliquots of CH_3CN at 90 ^{o}C (oil

bath) under a gentle stream of N_2. The resulting n-Bu$_4$N[^{18}F]F was dissolved in CH_3CN (100

μL) and transferred to a reaction vial containing the precursor **26** or **27** (0.35 μmol), and

stirred at 110 ^{o}C for 10 min. The reaction mixture was cooled, treated with 6 N HCl (200 μL),

and stirred at 120 ^{o}C for 10 min. The reaction mixture was cooled, diluted with water (2 mL),

and extracted with ethyl acetate (2 mL). The organic layer was washed with water and passed

through a 2-cm Na_2SO_4 plug, and solvent was removed under a stream of N_2 at 50 ^{o}C (water

bath). The crude product was then purified by HPLC using a semi-preparative column eluted

with a 65:35 (or 70:30) mixture of hexane and CH_2Cl_2 (containing 5% 2-propanol) at a flow

rate of 3.5 mL/min. The desired product eluted between 35 and 37 min (or 40 and 42 min)

was concentrated under a stream of N_2. For cellular uptake and microPET imaging studies,

the residue was re-dissolved in polysorbate 80 and diluted with saline to give a final solution

of 0.2% polysorbate 80 in saline.

Specific activity was determined by comparing UV peak areas of the desired radioactive

peak and those of different concentrations of unlabeled standard **1** or **2** on HPLC using an

analytical column eluted with a 45:55 mixture of water and acetonitrile each containing 0.1%

TFA at a flow rate of 1 mL/min. Identity of radioligand [^{18}F]**1** or [^{18}F]**2** was determined by

co-injecting the radioligand with the corresponding non-radioactive standard into the HPLC

system (see HPLC chromatograms, Supplementary Information).

Measurement of partition coefficient

Radioligand ((0.74 MBq) [^{18}F]**1** or [^{18}F]**2**) was added to a premixed suspension containing

600 μL of octanol and 600 μL of water, vortexed vigorously for 3 min, and then centrifuged.

Two layers were separated, and 100 μL aliquots of the octanol and aqueous layers were

removed and counted. Samples from the octanol and aqueous layers repartitioned until

consistent values were obtained. The experiments were conducted in triplicate. The log P is

expressed as the logarithm of the ratio of the counts per minute of octanol versus that of

water.

Cell lines and culture

HUVECs were maintained in endothelial cell growth medium-2 (EGM-2) (Lonza, Walkersville, MD, USA). Rat C6 glioma cells were cultured in Dulbecco's modified Eagle medium (DMEM) (Gibco, Brooklyn, NY, USA) supplemented with 10% fetal bovine serum (FBS) (Gibco) and 1% penicillin/streptomycin (Gibco). Cell lines were maintained at $37\,^{\circ}\mathrm{C}$ in a humidified 5% CO_2 incubator.

Animals

Animal study was reviewed and approved by the Institutional Animal Care and Use Committee of SBRI. SBRI is an Association for Assessment and Accreditation of Laboratory Animal Care International accredited facility and abide by the Institute of Laboratory Animal Resources Guide.

SRB assay

HUVEC and C6 glioma cells were seeded on 96-well plates at a density of 2×10^4 cells/well and incubated for 24 h to allow the cells to attach. The cells were treated with each of the compounds (0, 0.78, 1.56, 3.125, 6.25, 12.5, 25, 50, and 100 μM) for 72 h. All compounds were dissolved in a final concentration of 0.1% DMSO in media. After 72 h, the cells were

washed with PBS and fixed with 10% ice-cold trichloroacetic acid at 4 ^{o}C for 1 h. Fixed cells

were washed five times with distilled water, stained with 0.4% SRB in 1% acetic acid at

room temperature for 30 min, and then washed with 1% acetic acid. SRB-bound cells were

solubilized with 10 mM Tris buffer (pH 10.5), and the absorbance of the cells was read at a

wavelength of 515 nm on an ELISA microplate reader. The IC_{50} (50% inhibitory

concentration) values were calculated using GraphPad prism software.

Reduction with alcohol dehydrogenase

Reduction of **1** and **2** with alcohol dehydrogenase was performed as previously reported.[26,29]

The compound was dissolved in 0.1% DMSO in phosphate buffer (0.01 M, pH 7.4), and the

solution was pre-incubated with equine alcohol dehydrogenase (5 units/mL) at 37 ^{o}C for 3

min. The reaction was initiated by addition of NADPH (5 mM) at the same temperature. The

final volume was 0.5 mL. After 1 h, the incubation mixture was treated with acetate buffer (1

M, pH 4.5) and then extracted with a 9:1 mixture of ethyl acetate and 2-propanol. The organic

layer was dried, re-dissolved in HPLC solvents, and analyzed by HPLC using an analytical

column (YMC C18, 4.6 × 250 mm, 5 μm) and sequential gradients from a 95:5 mixture to a

55:45 mixture of 1% ammonium acetate in water (pH 4.5) and acetonitrile containing 0.05%

acetic acid over 30 min, followed by an increase to a 5:95 mixture over 20 min at a flow rate

of 1 mL/min. The eluent was monitored using a UV detector at 280 nm.

In vivo **metabolism studies in ICR mice**

[18F]**1** and [18F]**2** dissolved in 0.2% polysorbate 80 in saline were injected into ICR mice (male, 32-35 g) via a tail vein. At 5, 30, and 60 min after injection, mice were sacrificed, and samples of blood and liver were obtained, homogenized in 1 mL of ethanol, and centrifuged. The supernatants were passed through filters and then analyzed by HPLC using sequential gradients from a 95:5 mixture to a 55:45 mixture of 0.1% ammonium acetate in water (pH 4.5) and acetonitrile over 30 min, followed by an increase to a 5:95 mixture over 20 min at a flow rate of 1 mL/min. The eluents were monitored using a NaI(T1) radioactivity detector. In another experiment, the 5-min liver sample was incubated with β-glucuronidase in phosphate buffer (0.01 M, pH 7) at 37 °C for 30 min. The incubation mixture was homogenized in 1 mL of ethanol and centrifuged. The supernatant was analyzed by HPLC using the same conditions as described above.

Cellular uptake

HUVEC and C6 cells were seeded at 5×10^5 cells/well in 12-well plates and incubated for 24 h to allow the cells to attach. [18F]**1** or [18F]**2** (74 kBq) dissolved in polysorbate 80 (final

concentration: 0.1% in medium) was added to each well to give a total volume of 1 mL, and

the cells were incubated at 37 $^{\circ}$C for 5, 15, 30, 60, and 120 min. At the indicated time points,

cells were washed three times with PBS, lysed using 0.1 N NaOH, and the resulting lysate

was counted using a gamma counter. For blocking studies, the cells were incubated with

[^{18}F]**1** or [^{18}F]**2** (74 kBq) in the presence of 40 μM compound (**1** or **2**), curcumin, or HC at 37

$^{\circ}$C for 30 min and then treated as described above. All experiments were performed in

triplicate.

MicroPET imaging

C6 cells (2 × 10^6) were subcutaneously inoculated into the right hind legs of 5-week-old

BALB/c nude mice (male). When tumor size reached 255 ± 21 mm^3 at 2.5 weeks after

inoculation, [^{18}F]**1** or [^{18}F]**2** (7.4 MBq/200 μL) in 0.2% polysorbate 80 in saline was injected

intravenously into the mice through a tail vein (n=3). MicroPET images were acquired for 5

min at 30 and 60 min after injection. The images obtained were reconstructed using 3-D

ordered subset expectation maximization and then processed using Siemens Inveon Research

Workplace 4.1 (IRW 4.1). Regions of interest (ROIs) were drawn over tumors in the right

legs and the muscles in contralateral legs, and the average signal level in the ROIs was

measured**.**

Biodistribution

At the end of microPET imaging, 65 min after injection of radioligands, the mice were sacrificed. Blood and major tissues were removed, weighed, and their radioactivity counted. Data are expressed as the percent injected dose per gram of tissues (% ID/g).

Statistical analysis

The results were analyzed using unpaired, two-tailed Student's t-tests. Differences at the 95% confidence level ($P < 0.05$) were considered statistically significant.

Acknowledgements

Notes and references

1.   S. Shishodia, K. Misra and B. Aggarwal, in *Dietary Modulation of Cell Signaling Pathways*, ed. Y. J. Surh, Z. Dong, E. Cadenas and L. Packer, Press, Boca Raton, 2009, 4, 91-99.

2.   V. P. Menon and A. R. Sudheer, *Adv. Exp. Med. Biol.,* 2007, **595,** 105.

3.   P. Anand, A. B. Kunnumakkara, R. A. Newman and B. B. Aggarwal, *Mol. Pharm.*, 2007, **4**, 807.

4.   G. Shoba, D. Joy, T. Joseph, M. Majeed, R. Rajendran and P. Srinivas, *Planta Med.*, 1998, **64**, 353.

5.   S. S. Bansal, M. Goel, F. Aqil, M. V. Vadhanam and R. C. Gupta, *Cancer Prev. Res.*, 2011, **4**, 1158-1171.

6.   E. K. Ryu, Y. S. Choe, K.-H. Lee, Y. Choi and B.-T. Kim, *J. Med. Chem.*, 2006, **49**, 6111-6119.

7.   D. L. Flynn, T. R. Belliotti, A. M. Boctor, D. T. Connor, C. R. Kostlan, D. E. Nies, D. F. Ortwine, D. J. Schrier and J. C. Sircar, *J. Med. Chem.*, 1991, **34**, 518-525.

8.   C. Selvam, S. M. Jachak, R. Thilagavathi and A. K. Chakraborti, *Bioorg. Med. Chem. Lett.*, 2005, **15**, 1793.

9.   M. Mayadevi, D. Sherin, V. Keerthi, K. Rajasekharan and R. Omkumar, *Bioorg. Med.*

Chem., 2012, **20**, 6040.

10.   R. Narlawar, M. Pickhardt, S. Leuchtenberger, K. Baumann, S. Krause, T. Dyrks, S.

       Weggen, E. Mandelkow and B. Schmidt, *ChemMedChem*, 2008, **3**, 165.

11.   J. Ishida, H. Ohtsu, Y. Tachibana, Y. Nakanishi, K. F. Bastow, M. Nagai, H.-K. Wang,

       H. Itokawa and K.-H. Lee, *Bioorg. Med. Chem.*, 2002, **10**, 3481.

12.   J. S. Shim, D. H. Kim, H. J. Jung, J. H. Kim, D. Lim, S.-K. Lee, K.-W. Kim, J. W.

       Ahn, J.-S. Yoo and J.-R. Rho, *Bioorg. Med. Chem.*, 2002, **10**, 2439.

13.   X. Wang, Y. Zhang, X. Zhang, W. Tian, W. Feng and T. Chen, *Int. J. Oncol.*, 2012, **40**,

       1189.

14.   P. Elkins, D. Coleman, J. Burgess, M. Gardner, J. Hines, B. Scott, M. Kroenke, J.

       Larson, M. Lightner and G. Turner, *J. Pharm. Biomed. Anal.*, 2014, **88**, 174.

15.   J. Rokka, A. Snellman, C. Zona, B. La Ferla, F. Nicotra, M. Salmona, G. Forloni, M.

       Haaparanta-Solin, J. O. Rinne and O. Solin, *Bioorg. Med. Chem.* 2014, **22**, 2753.

16.   M. Asti, E. Ferrari, S. Croci, G, Atti, S. Rubagotti, M. Iori, P. C. Capponi, A. Zerbini,

       M. Saladini and A. Versari, *Inorg. Chem.* 2014, **53**, 4922.

17.   H. J. Koo, S. Shin, J. Y. Choi, K. H. Lee, B. T. Kim and Y. S. Choe, *Sci. Rep.* 2015, **5**,

       14205.

18.   H. Pabon, *Recueil des Travaux Chimiques des Pays-Bas*, 1964, **83**, 379.
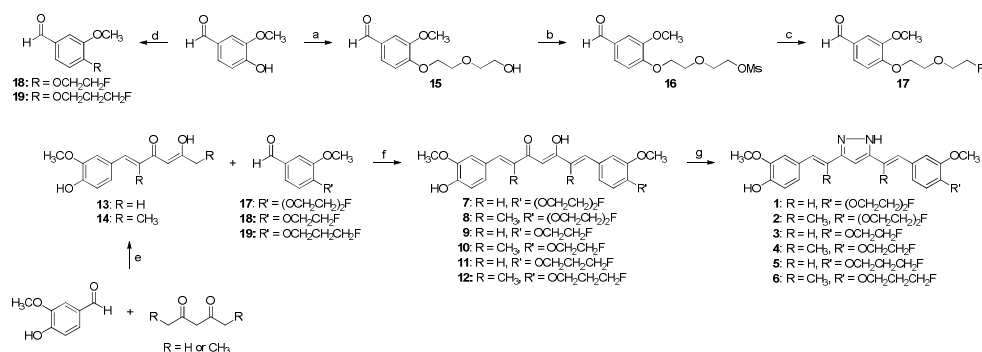
19.　　T. Masuda, H. Matsumura, Y. Oyama, Y. Takeda, A. Jitoe, A. Kida and K. Hidaka, *J. Nat. Prod.*, 1998, **61**, 609.

20.　　I. Lee, J. Yang, J. H. Lee and Y. S. Choe, *Bioorg. Med. Chem. Lett.*, 2011, **21**, 5765.

21.　　D. W. Kim, D.-S. Ahn, Y.-H. Oh, S. Lee, H. S. Kil, S. J. Oh, S. J. Lee, J. S. Kim, J. S. Ryu and D. H. Moon, *J. Am. Chem. Soc.*, 2006, **128**, 16394.

22.　　A. Bax and D. G. Davis, *J. Magn. Reson.,* 1985, **63**, 207.

23.　　E. Ämmälahti, M. Bardet, D. Molko and J. Cadet, *J. Magn. Reson. Series A*, 1996, **122**, 230.

24.　　P. Elkins, D. Coleman, J. Burgess, M. Gardner, J. Hines, B. Scott, M. Kroenke, J. Larson, M. Lightner and G. Turner, *J. Pharm. Biomed. Anal.*, 2014, **88**, 174.

25.　　J. Schleucher and S. S. Wijmenga, *J. Am. Chem. Soc.*, 2002, **124**, 5881.

26.　　S. I. Hoehle, E. Pfeiffer, A. M. Sólyom and M. Metzler, *J. Agric. Food Chem.*, 2006, **54**, 756.

27.　　C. R. Ireson, D. J. Jones, S. Orr, M. W. Coughtrie, D. J. Boocock, M. L. Williams, P. B. Farmer, W. P. Steward and A. J. Gescher, *Cancer Epidemiol. Biomarkers Prev.*, 2002, **11**, 105.

28.　　C. Ireson, S. Orr, D. J. Jones, R. Verschoyle, C.-K. Lim, J.-L. Luo, L. Howells, S. Plummer, R. Jukes and M. Williams, *Cancer Res.*, 2001, **61**, 1058.

29.   W. Zhang, S. Oya, M. P. Kung, C. Hou, D. L. Maier and H. F. Kung, *Nucl. Med. Biol.*, 2005, **32**, 799.

30.   W. Zhang, M. P. Kung, S. Oya, C. Hou and H. F. Kung, *Nucl. Med. Biol.*, 2007, **34**, 89.

31.   F. Van Heerden, J. Van Zyl, G. Rall, E. Brandt and D. Roux, *Tetrahedron Lett.*, 1978, **19**, 661.

32.   T. R. Kelly, C. T. Jagoe and Q. Li, *J. Am. Chem. Soc.*, 1989, **111**, 4522.

33.   S. I. Uehara, I. Yasuda, K. Akiyama, H. Morita, K. Takeya and H. Itokawa, *Chem. Pharm. Bull.*, 1987, **35**, 3298.

34.   M. H. Pan, T. M. Huang and J. K. Lin, *Drug Metab. Dispos.*, 1999, **27**, 486.

**Table 1** Cell viability of compounds **1-6**.

Cell lines	IC$_{50}$ (μM)							
	Curcumin	HC	**1**	**2**	**3**	**4**	**5**	**6**
HUVECs	7.18 ± 1.65	4.34 ± 1.35	5.88 ± 1.87	4.80 ± 1.31	9.77 ± 1.11	5.62 ± 1.52	10.84 ± 2.53	14.70 ± 1.13
C6 glioma cells	15.95 ± 0.98	4.52 ± 1.15	17.52 ± 1.59	16.35 ± 1.85	32.14 ± 2.12	22.25 ± 2.15	20.99 ± 2.18	25.25 ± 3.12

Data are mean ± SD from triplicate experiments.

Scheme 1 Synthesis of compounds **1-6**[a]

18: R = OCH$_2$CH$_2$F
19: R = OCH$_2$CH$_2$CH$_2$F

15 **16** **17**

13: R = H
14: R = CH$_3$

17: R' = (OCH$_2$CH$_2$)$_2$F
18: R' = OCH$_2$CH$_2$F
19: R' = OCH$_2$CH$_2$CH$_2$F

7: R = H, R' = (OCH$_2$CH$_2$)$_2$F
8: R = CH$_3$, R' = (OCH$_2$CH$_2$)$_2$F
9: R = H, R' = OCH$_2$CH$_2$F
10: R = CH$_3$, R' = OCH$_2$CH$_2$F
11: R = H, R' = OCH$_2$CH$_2$CH$_2$F
12: R = CH$_3$, R' = OCH$_2$CH$_2$CH$_2$F

1: R = H, R' = (OCH$_2$CH$_2$)$_2$F
2: R = CH$_3$, R' = (OCH$_2$CH$_2$)$_2$F
3: R = H, R' = OCH$_2$CH$_2$F
4: R = CH$_3$, R' = OCH$_2$CH$_2$F
5: R = H, R' = OCH$_2$CH$_2$CH$_2$F
6: R = CH$_3$, R' = OCH$_2$CH$_2$CH$_2$F

R = H or CH$_3$

[a]Reagents and conditions: (a) 2-(2-chloroethoxy)ethanol, K$_2$CO$_3$, DMF, 100 $^{\circ}$C, 5 h; (b) methanesulfonyl chloride, Et$_3$N, room temperature, 5 h; (c) CsF, *t*-BuOH, 100 $^{\circ}$C, 19 h; (d) 3-fluoroalkyltosylate, K$_2$CO$_3$, CH$_3$CN, 110 $^{\circ}$C, 3 h; (e) B$_2$O$_3$, ethyl acetate, (*n*-BuO)$_3$B, *n*-BuNH$_2$, 1 N HCl, 2.5 h; (f) B$_2$O$_3$, ethyl acetate, (*n*-BuO)$_3$B, piperidine, 0.4 N HCl, 3.5 h; (g) hydrazine hydrate, ethanol, acetic acid, 80 $^{\circ}$C, 18 h

Scheme 2 Synthesis of precursors (**26** and **27**) and radioligands ([^{18}F]**1** and [^{18}F]**2**)^a
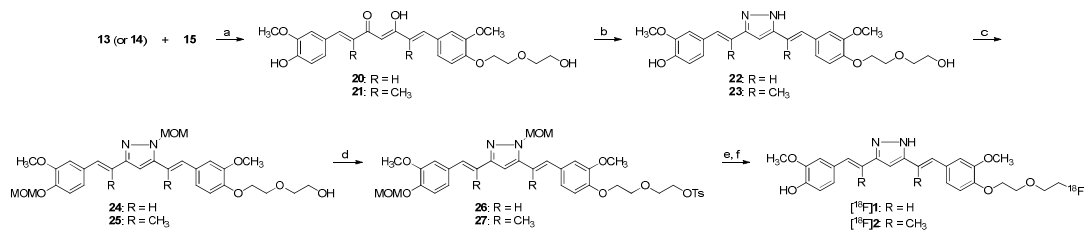
^{a}Reagents and conditions: (a) B$_2$O$_3$, ethyl acetate, (*n*-BuO)$_3$B, *n*-BuNH$_2$, 1 N HCl, 3.5 h; (b)

hydrazine hydrate, EtOH, acetic acid, 80 ^{o}C, 18 h; (c) chloromethyl methyl ether, 2 N NaOH,

Adogen 464, CH$_2$Cl$_2$, room temperature, 20 min; (d) TsCl, Et$_3$N, CH$_2$Cl$_2$, room temperature,

20 h; (e) *n*-Bu$_4$N^{18}F, CH$_3$CN, 110 ^{o}C, 10 min; (f) 6 N HCl, 120 ^{o}C, 10 min

Figure legends

Fig. 1 Chemical structures of curcumin, HC, and fluorine-substituted HC derivatives (**1-6**).

Fig. 2 Reduction of **1** and **2** with alcohol dehydrogenase. Compounds were incubated with alcohol dehydrogenase and NADPH at 37 °C for 1 h and the incubation mixture was analyzed by HPLC at 280 nm. (A) **1**; (B) **1** + alcohol dehydrogenase + NADPH; (C) alcohol dehydrogenase; (D) **2**; (E) **2** + alcohol dehydrogenase + NADPH; (F) **2** + alcohol dehydrogenase; (G) curcumin; (H) curcumin + alcohol dehydrogenase + NADPH; (I) authentic tetrahydrocurcumin

Fig. 3 *In vivo* metabolism study of (A) [^{18}F]**1** and (B) [^{18}F]**2** in ICR mice. Samples of blood and liver were extracted, homogenized, and centrifuged. The supernatants were analyzed by HPLC using a NaI(T1) radioactivity detector: (a) parent radioligand; (b) blood sample at 5 min after injection; (c) liver sample at 5 min; (d) liver sample at 30 min; (e) liver sample at 5 min + β-glucuronidase

Fig. 4 Comparison of cellular uptake of [^{18}F]**1** and [^{18}F]**2**. (A) HUVEC uptake of [^{18}F]**1** as a function of time and (B) after co-incubation with **1**, curcumin, or HC for 30 min; (C) C6 cellular uptake of [^{18}F]**1** and (D) after co-incubation with **1**, curcumin, or HC for 30 min. (E) HUVEC uptake of [^{18}F]**2** as a function of time and (F) after co-incubation with **2**, curcumin, or HC for 30 min; (G) C6 cellular uptake of [^{18}F]**2** and (H) after co-incubation with **2**, curcumin, or HC for 30 min. Cellular uptake levels are expressed as a function of time relative to a value of 100 % at 5 min. $^{*}P < 0.05$, $^{**}P < 0.01$, and $^{***}P < 0.001$.

Fig. 5 MicroPET images of (A) [^{18}F]**1** and (B) [^{18}F]**2** in a C6 glioma xenograft model. (C) ROI analysis of the tumor uptake at 30 min and 60 min after injection of [^{18}F]**1** (white) and [^{18}F]**2** (black). Dotted circles indicate tumors. $^{**}P < 0.01$ and $^{***}P < 0.001$.

Fig. 6 Biodistribution of [^{18}F]**1** (white) and [^{18}F]**2** (black) in a C6 glioma xenograft model at 65 min post-injection. Inset is an enlarged graph showing tumor uptake of [^{18}F]**1** (white) and [^{18}F]**2** (black). I indicates intestine. Values (% ID/g) are given as the means ± SD of each group (n = 3). $^{*}P < 0.05$ and $^{**}P < 0.01$.

Fig. 1
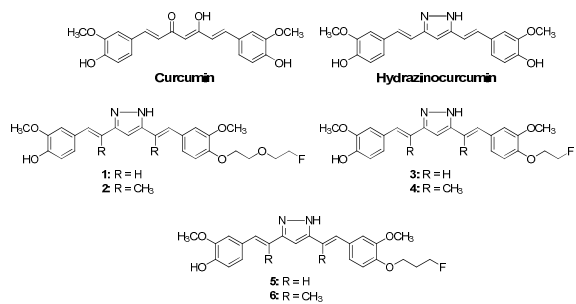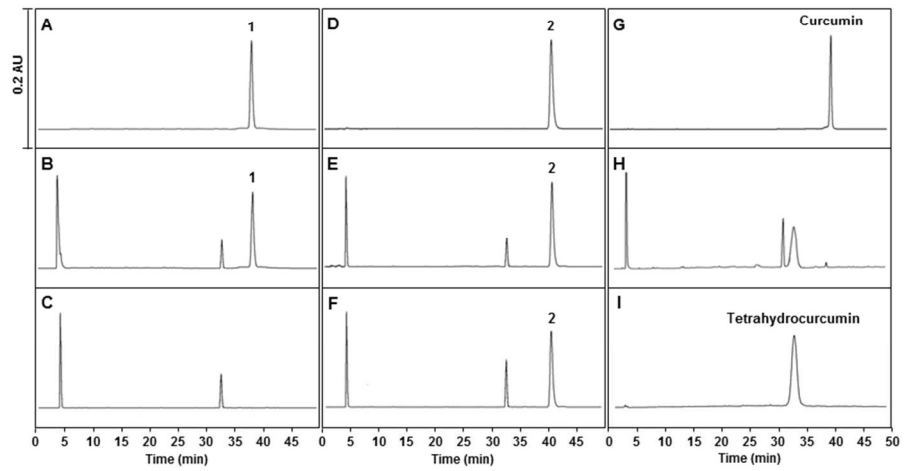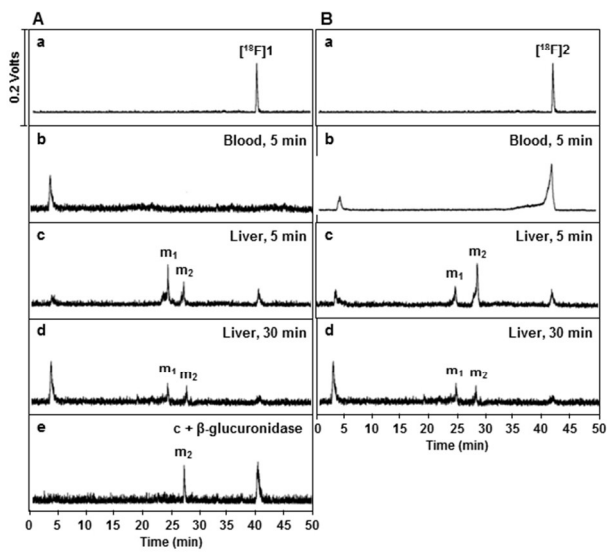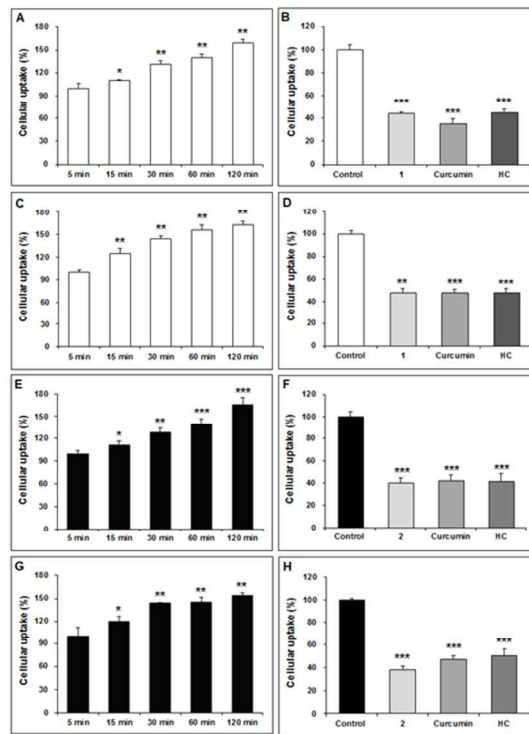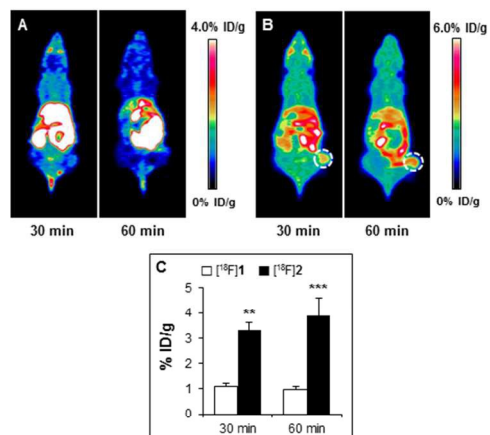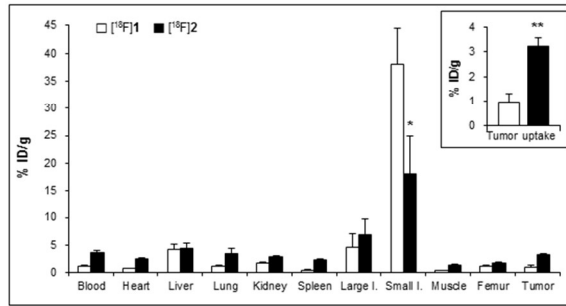
254x190mm (96 x 96 DPI)

254x190mm (96 x 96 DPI)

254x190mm (96 x 96 DPI)

254x190mm (96 x 96 DPI)

254x190mm (96 x 96 DPI)